

Universal Finite Size Scaling Functions in the 3D Ising Spin Glass

Matteo Palassini

*Department of Physics, University of California, Santa Cruz, California 95064
Scuola Normale Superiore and INFN, 56100 Pisa, Italy*

Sergio Caracciolo

*Scuola Normale Superiore and INFN, 56100 Pisa, Italy
(Submitted February 10, 1999)*

We study the three-dimensional Edwards–Anderson model with binary interactions by Monte Carlo simulations. Direct evidence of finite-size scaling is provided, and the universal finite-size scaling functions are determined. Monte Carlo data are extrapolated to infinite volume with an iterative procedure up to correlation lengths $\xi \approx 140$. The infinite volume data are consistent with a conventional power law singularity at finite temperature T_c . Taking into account corrections to scaling, we find $T_c = 1.156 \pm 0.015$, $\nu = 1.8 \pm 0.2$ and $\eta = -0.26 \pm 0.04$. The data are also consistent with an exponential singularity at finite T_c , but not with an exponential singularity at zero temperature.

PACS numbers: 75.10.Nr, 64.60.Fr, 75.40.Mg, 75.50.Lk

The critical properties of the Ising spin glass in three dimensions are still not very well understood. Numerical simulations have led to some progress [1,2], but have been hampered by technical difficulties. Large-scale Monte Carlo (MC) simulations at correlation length $\xi \approx 10$ lattice units [3–5] are consistent with both a continuous phase transition with power-law divergence of ξ at finite temperature $T = T_c$, and an exponential divergence at $T = 0$, which is expected at the lower critical dimension. High-statistics MC simulations of smaller systems [6–8] give a certain evidence of a $T_c \neq 0$ transition with an ordered spin glass phase below T_c , but cannot exclude neither an exponential divergence at $T = 0$, nor a line of critical points at $T \leq T_c \neq 0$ [6,8,9], as in the Kosterlitz–Thouless theory of the 2D XY model. Understanding whether an ordered spin glass phase exists in three dimensions is clearly an issue of major interest.

In this work, we study the 3D Ising spin glass with an approach, based on finite-size scaling (FSS) and MC simulations in the paramagnetic phase, introduced in Ref. [10] (see Ref. [11] for similar methods) and so far applied to non-disordered systems. Let us summarize our main results. (i) We provide a direct test of the FSS hypothesis, independent of the nature of the divergence in the infinite system. In particular we determine, for the first time to our knowledge, the *universal* FSS functions. (ii) We demonstrate the effectiveness of an iterative procedure to extrapolate the MC data to infinite volume, that allows us to reach $\xi \approx 140$. (iii) Exploiting the higher range of ξ , we show that an exponential divergence at $T = 0$ is excluded, but we still cannot decide between a power-law divergence at $T_c \neq 0$ and a line of critical points terminating at $T_c \neq 0$. (iv) Under the hypothesis of power-law divergence, we show that corrections to scaling are important and we estimate T_c and the critical exponents.

Model and FSS method — We consider the 3D Edwards–Anderson model, whose Hamiltonian is

$$\mathcal{H} = - \sum_{\langle xy \rangle} \sigma_x J_{xy} \sigma_y \quad (1)$$

where σ_x are Ising spins on a simple cubic lattice of linear size L with periodic boundaries, and J_{xy} are independent random interactions taking the values ± 1 with probability $\frac{1}{2}$. The sum runs over pairs of nearest neighbor sites.

Let $\xi(T, L)$ be a suitably defined finite-volume correlation length, and let $\mathcal{O}(T, L)$ be any singular observable, such as $\xi(T, L)$ itself or the spin-glass susceptibility (see below). Then FSS theory [12] predicts that

$$\frac{\mathcal{O}(T, L)}{\mathcal{O}(T, \infty)} = f_{\mathcal{O}}(\xi(T, \infty)/L) , \quad (2)$$

where $f_{\mathcal{O}}$ is a universal function and corrections to FSS are neglected. From Eq. (2) one obtains the relation

$$\frac{\mathcal{O}(T, 2L)}{\mathcal{O}(T, L)} = F_{\mathcal{O}}(\xi(T, L)/L) , \quad (3)$$

where $F_{\mathcal{O}}$ is another universal function and only finite-volume observables are involved. Our approach works as follows (see Ref. [10] for details). We make MC runs at numerous pairs (T, L) , $(T, 2L)$ and we plot $\mathcal{O}(T, 2L)/\mathcal{O}(T, L)$ versus $\xi(T, L)/L$. If all these points fall with good accuracy on a single curve — thus verifying the Ansatz (3) — we choose a smooth fitting function $F_{\mathcal{O}}$. Then, using the functions F_{ξ} and $F_{\mathcal{O}}$, we extrapolate the pair (ξ, \mathcal{O}) iteratively from $L \rightarrow 2L \rightarrow 2^2L \rightarrow \dots \rightarrow \infty$.

Computational details — We simulate the model in Eq.(1) with the heath–bath algorithm. We measure $q_x = \sigma_x \tau_x$ and $q = L^{-3} \sum_x q_x$ from two independent replicas (σ, τ) with the same J_{xy} . We choose as a definition of $\xi(T, L)$ the *second-moment* correlation length

$$\xi(T, L) = \frac{[S(0)/S(p) - 1]^{1/2}}{2 \sin(|p|/2)} \quad (4)$$

where $S(k)$ is the Fourier transform

$$S(k) = \sum_r e^{ik \cdot r} \langle q_x q_{x+r} \rangle, \quad (5)$$

(arguments T, L are omitted) and $p = (0, 0, 2\pi/L)$ is the smallest non-zero wave vector [13]. The spin-glass susceptibility is $\chi_{SG}(T, L) \equiv L^3 \langle q^2 \rangle = S(0)$. The symbol $\langle \cdot \rangle$ represents a double average over thermal noise and J_{xy} , which is estimated from N_s samples with different J_{xy} .

The runs are done on a Cray T3E parallel computer with a fast code that exploits the parallelism of spin glass simulations. The binary variables σ_x and J_{xy} at corresponding sites of 64 samples (each represented by a single bit) are stored in a 64-bit integer variable, and 64 σ_x 's are updated simultaneously with only 31 logical instructions and one random number [14]. Average speed on a single processor (PE) is 4.5×10^7 spin updates per second (DEC Alpha EV5, 600 MHz). The PEs are arranged in a virtual parallelepiped along whose axis we can distribute independent groups of 64 samples, different ‘‘slices’’ of a large lattice, and different temperatures. We typically used 32 to 128 PEs. Equilibration of the runs is verified with the criterion introduced in Ref. [15]. The sizes simulated range from $L = 4$ to $L = 48$, from which we form 104 pairs (T, L) , $(T, 2L)$. In Table I some parameters of the simulations are given. The equivalent of about 2 years of computer time on a single PE was employed.

TABLE I. Maximum number of samples N_s , minimum temperature T_m and Monte Carlo sweeps (MCS) performed at T_m , as a function of the size L .

L	4 - 8	10	12	16	24	32	48
N_s	1920	1536	960	448	448	448	64
T_m	.9401	.9793	1.0936	1.1642	1.2059	1.3397	1.4084
MCS/ 10^6	3	10	10	10	10	10	10

FSS analysis — In Fig. 1 we show that, within our statistical accuracy, the FSS Ansatz (3) is well verified for $\mathcal{O} = \chi_{SG}$ and $\mathcal{O} = \xi$. No systematic deviations from the curves are detectable, but data at $L = 4$, not displayed in Fig. 1, are significantly outside the curves for $\xi(T, L)/L \equiv x > 0.2$. We verified that other observables, such as the Binder ratio, also satisfy Eq.(3). We emphasize that FSS was not assumed *a priori* and that Eq.(3) contains no adjustable parameters. Furthermore, no particular dependence of ξ and χ_{SG} on T was assumed.

We fit the data in Fig. 1 to two functions $F_{\chi_{SG}}, F_{\xi}$ of the form $F(x) = 1 + \sum_{i=1, n} a_i \exp(-i/x)$, obtaining good fits with $n = 3$ or 4 (*goodness of fit* parameter $Q > 0.9$). Using $F_{\chi_{SG}}, F_{\xi}$, we then compute $\chi_{SG}(T, \infty)$, $\xi(T, \infty)$

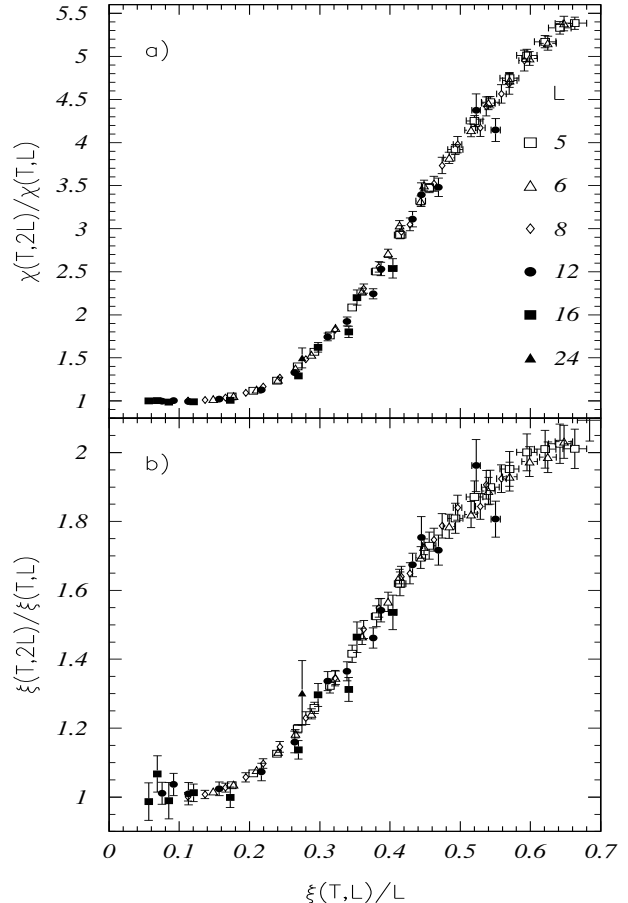


FIG. 1. Finite-size-scaling plot with the form in Eq.(3) for a) $\mathcal{O} = \chi_{SG}$ and b) $\mathcal{O} = \xi$. Error bars (estimated with a jackknife procedure) are one standard deviation.

with the iterative procedure described above. In Table II we show that extrapolations from different L are consistent, providing a test of the method. In our final analysis, we take the weighted average of the extrapolations from different L . An implicit assumption of the iterative procedure is that the Ansatz (3) with a given function $F_{\mathcal{O}}$ will continue to hold as $L \rightarrow \infty$. This assumption could fail if the system exhibits a crossover at large L , as in any FSS analysis. However, as shown in Table II, extrapolations at $T = 1.4084$ from small L are consistent with data from large L , which have little or no finite-size effects. We therefore believe that a crossover is unlikely.

In order to test for systematic errors due to corrections to FSS, we repeated the analysis excluding $L = 5, 6$ from the fits of $F_{\chi_{SG}}, F_{\xi}$ and we found that extrapolated data change within their error bars. We have a good control on the extrapolated data up to $\xi \approx 140$; at lower temperatures the statistical errors become quite large, and the data are more sensitive to the region of high x , where there are few data from large L . (The largest x used for the extrapolations is $x = 0.57$, from $T = 1.2059, L = 5$).

In Fig. 2 we show that with our extrapolated data

Eq.(2) is satisfied remarkably well, providing a further test of the method. If $\mathcal{O} \sim \xi^{\gamma_{\mathcal{O}}/\nu}$ as $\xi \rightarrow \infty$, then $f_{\mathcal{O}}(x)$ in Eq.(2) must satisfy $f_{\mathcal{O}}(x) \sim x^{-\gamma_{\mathcal{O}}/\nu}$ as $x \rightarrow \infty$. As shown in Fig. 2 (insets), our curves indeed have a power-law asymptotic decay, with negative slopes $\gamma/\nu = 2.30 \pm 0.08$ in Fig. 2(a) and ≈ 1 in Fig. 2(b).

We emphasize the *universality* of the scaling functions in Fig. 1 and 2. It would be interesting to determine the same functions for different distributions of the J_{xy} , in order to test for possible violations of universality [16,17].

TABLE II. Examples of measured and extrapolated values of the correlation length and the spin-glass susceptibility. See Ref. [10] for how to estimate error bars of extrapolated values.

T	L	$\xi(T, L)$	$\xi(T, \infty)$	$\chi_{SG}(T, L)$	$\chi_{SG}(T, \infty)$
1.2059	5	2.85(7)	120(60)	36.1(3)	$1.8(5) \times 10^9$
	6	3.42(6)	150(60)	55.1(5)	$2.8(8) \times 10^5$
	8	4.47(6)	126(30)	103(1)	$1.9(5) \times 10^5$
	10	5.57(6)	146(30)	171(2)	$2.8(8) \times 10^5$
	12	6.60(8)	143(30)	260(3)	$2.7(8) \times 10^5$
	16	8.60(15)	131(30)	473(10)	$2.1(8) \times 10^5$
1.4084	5	2.28(5)	8.5(9)	25.4(2)	$4.3(3) \times 10^2$
	6	2.66(4)	8.7(7)	36.1(4)	$4.6(3) \times 10^2$
	8	3.33(4)	8.4(4)	60.0(6)	$4.3(2) \times 10^2$
	10	3.94(4)	8.4(3)	88.3(1)	$4.3(2) \times 10^2$
	12	4.51(5)	8.6(3)	120(2)	$4.5(2) \times 10^2$
	16	5.46(8)	8.6(3)	178(4)	$4.4(2) \times 10^2$
	24	6.60(11)	8.1(2)	269(6)	$4.2(2) \times 10^2$
	32	7.16(15)	7.8(2)	320(9)	$3.8(2) \times 10^2$
	48	8.6(6)	8.9(7)	404(30)	$4.3(3) \times 10^2$

Nature of the phase transition — We now compare our extrapolated data with the following scenarios: (i) a $T_c \neq 0$ continuous phase transition; (ii) a line of critical points terminating at $T_c \neq 0$, with an exponential divergence as $T \rightarrow T_c^+$; (iii) an exponential divergence at $T = 0$. The last two scenarios imply a lower critical dimension exactly equal to three.

(i) We fit our data to

$$\xi(T) = c_{\xi} (T - T_c)^{-\nu} [1 + a_{\xi} (T - T_c)^{\theta}] \quad (6)$$

$$\chi_{SG}(\xi) = b \xi^{2-\eta} [1 + d \xi^{-\Delta}] \quad (7)$$

with fixed correction-to-scaling exponents θ and Δ [18]. In the fit we include data with $\xi \geq \xi_m$, varying ξ_m in order to test the stability of the fits. Without the corrections to scaling ($a_{\xi} = d = 0$), the quality of fits is good for $\xi_m > 3 - 4$ ($Q \approx 1$), but fit parameters (noticeably T_c, ν and η) show small *systematic* variations with ξ_m in the whole range available. Including the corrections, we obtain excellent and stable fits with $1 \leq \theta \leq 2$ and $1 \leq \Delta \leq 1.5$, the preferred values being $\theta = 1.4$ ($Q > 0.6$) and $\Delta = 1.3$ ($Q > 0.98$). Our estimates for the fitting parameters are $T_c = 1.156 \pm 0.015$, $\nu = 1.8 \pm 0.2$,

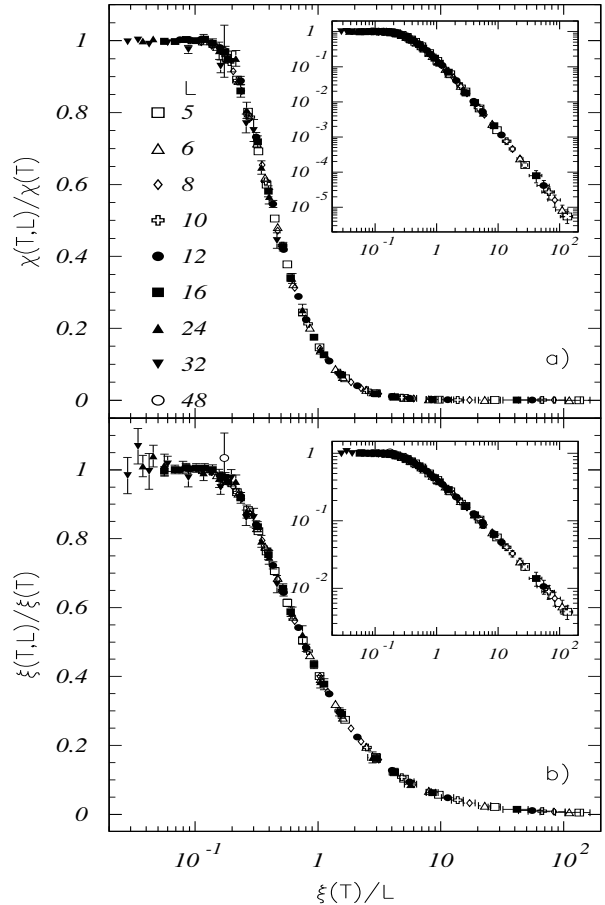


FIG. 2. Finite-size-scaling plot with the form in Eq.(2) for a) $\mathcal{O} = \chi_{SG}$ and b) $\mathcal{O} = \xi$. The insets represent the same data in a log-log plot, showing power-law decay for large ξ/L .

$\eta = -0.26 \pm 0.04$, $c_{\xi} = 0.7 \pm 0.2$, $a_{\xi} = 0.5 \pm 0.3$, $b = 3.3 \pm 0.3$ and $d = 0.9 \pm 0.1$, where the errors take into account the uncertainties on θ and Δ . We then obtain $\gamma = \nu(2 - \eta) = 4.1 \pm 0.5$. As shown in Fig. 3 and 4, corrections to scaling are important for $\xi \leq 10$ [19]. Since the fits do not include the *analytic* corrections to scaling, Δ and θ should be regarded as “effective” exponents. For comparison, we quote some estimates from other MC works: $T_c = 1.175 \pm 0.025$ [4], 1.11 ± 0.04 [6], 1.13 ± 0.06 [8], 1.19 ± 0.01 [17]; $\nu = 1.3 \pm 0.1$ [4], 1.20 ± 0.04 [5], 1.7 ± 0.3 [6], 2.00 ± 0.15 [7], 1.33 ± 0.05 [17]; $\eta = -0.22 \pm 0.05$ [4], -0.35 ± 0.05 [6], -0.30 ± 0.06 [7], -0.37 ± 0.04 [8], -0.22 ± 0.02 [17] (notice that in Ref. [7] a gaussian distribution of the bonds was considered).

(ii) We fit our data to

$$\xi(T) = f_{\xi} \exp(g_{\xi}/(T - T_c)^{\sigma}) \quad (8)$$

testing the fit stability as above. The fits are excellent with $\xi_m \geq 1.3$ but, due to strong correlations between σ and T_c , the errors on the fit parameters are large. For $\xi_m = 1.9$ the best fit gives $\sigma = 0.20 \pm 0.05$,

$T_c = 1.13 \pm 0.02$, $f_\xi = (1.0 \pm 0.2) \times 10^{-3}$, $g_\xi = 7 \pm 2$ ($Q = 0.77$). Notice, however, that any power-law can be approximated by an exponential with sufficiently small σ . For $\xi_m = 3.8$ the best fit (shown in Fig. 4) gives $\sigma = 0.5 \pm 0.3$, $T_c = 1.08 \pm 0.04$, $f_\xi = (1.1 \pm 0.8) \times 10^{-1}$, $g_\xi = 2.4 \pm 1.5$ ($Q = 0.69$). The deviations of the data from this fit for $\xi < 3$ are consistent with corrections to scaling of $\approx 10\%$. In general, in the presence of an exponential singularity we expect multiplicative logarithmic corrections to Eq.(7). Our data fit well to

$$\chi_{SG}(\xi) = b_l \xi^{2-\eta} (\log \xi)^r \quad (9)$$

for $\xi_m > 2$, giving $b_l = 1.30 \pm 0.03$, $\eta_l = -0.36 \pm 0.03$, $r = -0.36 \pm 0.06$ ($Q > 0.9$) (see also Fig. 3).

(iii) When we fit our data to

$$\xi(T) = f_\xi \exp(g_\xi/T^\sigma) \quad (10)$$

we find that σ increases continuously with ξ_m , from $\sigma \approx 3$ to $\sigma \approx 9$ [20]. Even assuming that σ stabilizes for higher ξ , we believe that a value $\sigma > 9$ is implausibly large. In fact, Eq. (10) implies a renormalization group (RG) transformation $dT/dl \propto T^{\sigma+1}$ (e^l being the RG scale factor), while for $T \rightarrow 0$ (at the lower critical dimension) we expect $dT/dl = a_2 T^2 + a_3 T^3 + \dots$ ($a_2 = 0$ in the phenomenological RG theory of Ref. [21]).

To conclude, we have shown that FSS is verified in the 3D Ising spin glass and that the correlation length diverges at a *finite* temperature. Whether this is a conventional continuous phase transition (in which case the lower critical dimension is probably close to three) or a transition to a line of critical points, is still not known.

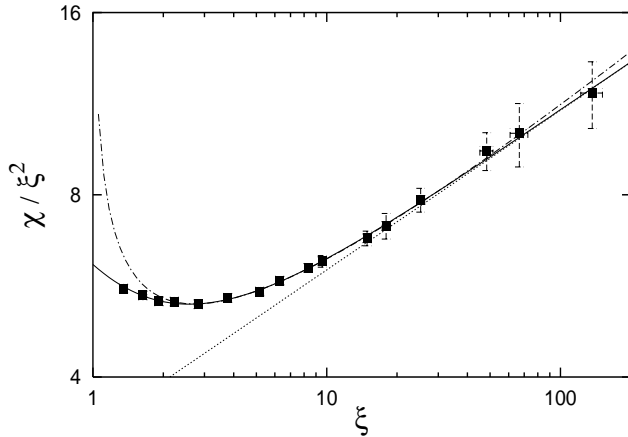


FIG. 3. Critical behavior of the infinite volume data. The solid line is the best fit to Eq.(7) for $\xi \geq 1.8$, the dotted line is the leading term from the same fit, the dot-dashed line is the best fit to Eq.(9) for $\xi \geq 2.2$.

We thank A. Pelissetto, A.P. Young and O.C. Martin for useful discussions. This work was supported by the INFM Parallel Computing Initiative.

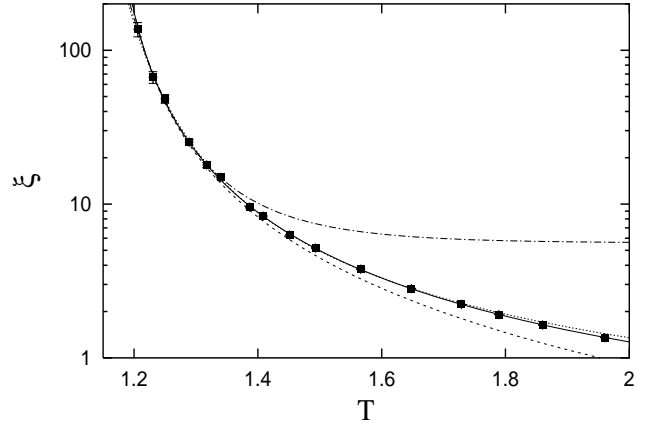


FIG. 4. Critical behavior of the infinite volume data. The solid line is the best fit to Eq.(6) for $\xi \geq 1.9$, the dotted line is the leading term from the same fit, the dashed line is the best fit to Eq.(8) for $\xi \geq 3.8$, the dot-dashed line is the best fit to Eq.(10) for $\xi \geq 14$.

- [1] K. Binder and A.P. Young, Rev. Mod. Phys. **58**, 801 (1986).
- [2] E. Marinari, G. Parisi and J. Ruiz-Lorenzo, in *Spin Glasses and Random Fields*, edited by A. P. Young (World Scientific, Singapore, 1997).
- [3] A.T. Ogielski and I. Morgenstern, Phys. Rev. Lett. **54**, 928 (1985).
- [4] A.T. Ogielski, Phys. Rev. B **32**, 7384 (1985).
- [5] E. Marinari, G. Parisi and F. Ritort, J. Phys. A **27** (1994).
- [6] N. Kawashima and A.P. Young, Phys. Rev. B **53**, R484 (1996).
- [7] E. Marinari, G. Parisi and J.J. Ruiz-Lorenzo, Phys. Rev. B **58**, 14852 (1998).
- [8] B.A. Berg and W. Janke, Phys. Rev. Lett. **80**, 4771 (1998); W. Janke, B.A. Berg and A. Billoire, cond-mat/9811423.
- [9] D. Iniguez, E. Marinari, G. Parisi and J.J. Ruiz-Lorenzo, J. Phys. A **30** 7337 (1997).
- [10] S. Caracciolo, R.G. Edwards, S.J. Ferreira, A. Pelissetto and A.D. Sokal, Phys. Rev. Lett. **74**, 2969 (1995).
- [11] M. Lüscher, P. Weisz, and U. Wolff, Nucl. Phys. **B359**, 221 (1991); J.-K. Kim, Phys. Rev. Lett. **70**, 1735 (1993).
- [12] M.N. Barber, in *Phase Transitions and Critical Phenomena*, vol. 8, edited by C. Domb and J.L. Lebowitz (Academic Press, London, 1983).
- [13] Eq.(4) is one of the possible definitions giving $\xi(T, \infty) = \left(\frac{1}{2D} \sum_x |x|^2 G(x) / \sum_x G(x)\right)^{\frac{1}{2}}$, where $G(x-y) = \langle q_x q_y \rangle$.
- [14] N. Kawashima, N. Ito and Y. Kanada, Int. J. Mod. Phys. C **4**, 525 (1993).
- [15] R.N. Bhatt and A.P. Young, Phys. Rev. E **37**, 5606 (1985).
- [16] L.W. Bernardi, S. Prakash and I.A. Campbell, Phys. Rev. Lett. **77**, 2798 (1996).
- [17] P.O. Mari and I.A. Campbell, Phys. Rev. E **59**, 2653 (1999).
- [18] In practice the fits are performed using the logarithm of both sides of Eqs. (6,7). The same is true for Eqs. (8,9,10).
- [19] Fits to $\chi_{SG}(T) = c_\chi (T-T_c)^{-\gamma} [1+a_\chi (T-T_c)^\theta]$ are much

less stable, due to stronger corrections to scaling ($> 100\%$ for $T > 1.5$). For $\xi_m > 9$ we find $T_c = 1.14 \pm 0.03$, $\gamma = 4.4 \pm 0.6$, $c_\chi = 0.7 \pm 0.5$, $a_\chi = 5 \pm 6$.

[20] With $1 \leq \xi \leq 9.6$ we get $\sigma = 3.1 \pm 0.1$, similarly to Refs. [4,5] where the largest ξ considered was $\xi \approx 10$.

[21] W.L. McMillan, J. Phys. C **17**, 3179 (1984).